

Robustness analysis of binary-coupled logistics-supply chain interdependent networks under load redistribution

Hai-Bo Yu(于海波), Yan-Li Gao(高彦丽), Guang-Ming Chen(陈光明), Qiu-Yu Tang(唐秋宇), Chao Feng(凤超), and Lei Zhang(张雷)

Citation: Chin. Phys. B, 2026, 35 (**7**): 078902. DOI: 10.1088/1674-1056/ae6432
http://cpb.iphy.ac.cn; http://iopscience.iop.org/cpb

What follows is a list of articles you may be interested in

Evolutionary hypergraph dismantling via deep reinforcement learning

Junjie Qian(钱俊杰), Wenlan Wang(王文蓝), Hanyun Wang(王涵韵), Qiqi Wang(王萁淇), Yao Zhang(张瑶), and Huijia Li(李慧嘉)

Chin. Phys. B, 2026, 35 (**6**): 068901. DOI: 10.1088/1674-1056/ae5a12

Robustness of community networks against cascading failures with heterogeneous redistribution strategies

Bo Song(宋波), Hui-Ming Wu(吴惠明), Yu-Rong Song(宋玉蓉), Guo-Ping Jiang(蒋国平),Ling-Ling Xia(夏玲玲), and Xu Wang(王旭)

Chin. Phys. B, 2023, 32 (**9**): 098905. DOI: 10.1088/1674-1056/acd9c3

Percolation transitions in edge-coupled interdependent networks with directed dependency links

Yan-Li Gao(高彦丽), Hai-Bo Yu(于海波), Jie Zhou(周杰), Yin-Zuo Zhou(周银座), and Shi-Ming Chen(陈世明)

Chin. Phys. B, 2023, 32 (**9**): 098902. DOI: 10.1088/1674-1056/acd685

Cascading failures of overload behaviors using a new coupled network model between edges

Yu-Wei Yan(严玉为), Yuan Jiang(蒋沅), Rong-Bin Yu(余荣斌), Song-Qing Yang(杨松青), and Cheng Hong(洪成)

Chin. Phys. B, 2022, 31 (**1**): 018901. DOI: 10.1088/1674-1056/ac1337

Cascading failure in multilayer networks with dynamic dependency groups

Lei Jin(金磊), Xiaojuan Wang(王小娟), Yong Zhang(张勇), Jingwen You(由婧文)

Chin. Phys. B, 2018, 27 (**9**): 098901. DOI: 10.1088/1674-1056/27/9/098901

Robustness analysis of binary-coupled logistics–supply chain interdependent networks under load redistribution

Hai-Bo Yu(于海波)[1], Yan-Li Gao(高彦丽)[2], Guang-Ming Chen(陈光明)[2], Qiu-Yu Tang(唐秋宇)[1], Chao Feng(凤超)[1], and Lei Zhang(张雷)[3,†]

[1] *School of Economics and Management, Xinjiang Institute of Technology, Aksu* 843100, *China*
[2] *School of Electrical and Automation Engineering, East China JiaoTong University, Nanchang* 330013, *China*
[3] *School of Management, Zhejiang University of Finance & Economics, Hangzhou* 310018, *China*

(Received 30 January 2026; revised manuscript received 17 April 2026; accepted manuscript online 24 April 2026)

To capture the interdependencies between logistics and supply chain networks in real-world systems, this paper develops a load redistribution-based logistics–supply chain binary-coupled network (LSBCN) model. Employing a dynamic load redistribution strategy, we systematically investigate the robustness of the LSBCN under cascading failures. We evaluate network performance under both random and deliberate failures, thoroughly analyze the mechanisms of influence of capacity factor (β) and capacity index (γ) on network robustness, and design three optimization strategies: parameter optimization, critical edge protection, and redundant edge addition. Furthermore, we quantitatively examine the synergistic effects and cost-effectiveness among these strategies. The results reveal that capacity factors exert significant regulatory effects on network robustness; however, the marginal improvement diminishes beyond a critical threshold. Distinct optimal capacity parameter configurations correspond to different failure proportions. Protecting critical edges of the logistics network demonstrates superior robustness enhancement under random failures, whereas adding redundant edges proves more effective under deliberate failures. The synergistic effects between strategies exhibit strong dependence on both failure modes and proportions. Under random failures, critical edge protection should be prioritized, while under deliberate failures, redundant edge addition is preferable. These findings provide theoretical foundations and decision-making references for vulnerability assessment, collaborative optimization, and risk management in logistics–supply chain systems.

Keywords: binary-coupled, logistics–supply chain networks, load redistribution, cascading failure, robustness analysis

PACS: 89.75.–k, 89.75.Fb, 64.60.ah

DOI: 10.1088/1674-1056/ae6432 **CSTR:** 32038.14.CPB.ae6432

1. Introduction

As the core region of the "Belt and Road" initiative and a critical node along the Eurasian golden corridor, Xinjiang's modern logistics and supply chain system serves as strategic infrastructure connecting production networks in central and western China with Eurasian consumer markets. The "channel + hub + network" modern logistics operation system established in Xinjiang not only supports the transformation and upgrading of the region's eight major industrial clusters but also provides essential logistical support for national energy resource transportation and high-quality agricultural and livestock product distribution. Furthermore, the deep synergistic capabilities of supply chain networks enable precise matching between supply and demand, effectively reducing resource misallocation and facilitating Xinjiang's integration into the national unified market.[1,2] However, the deep coupling between logistics and supply chain systems also exposes them to risks of cascading failure. Investigating the robustness of these systems holds significant practical implications for ensuring the smooth economic circulation in Xinjiang and enhancing the resilience of the industrial chain.

Real-world systems such as supply chain networks, logistics networks, energy networks, transportation networks, and communication networks can all be abstracted as complex network models with specific topological structures and functions.[3–5] The rapid development of information technology has enabled these networks to expand dramatically in scale, with increasingly prominent coupling relationships between them. Existing research indicates that such interdependencies tightly integrate different network systems to maintain coordinated operation; however, localized failures can propagate across multiple networks through these dependency relationships, leading to cascading failures or even systemic collapse, thereby substantially aggravating network vulnerability.[6–10] Risks of cascading failure arising from network interdependencies have become increasingly prevalent in recent years. For instance, the global COVID-19 pandemic in 2020 disrupted logistics and economic network operations, causing severe impacts and losses across numerous industries.[11,12] In 2021, extreme cold weather in Texas triggered large-scale power outages, which subsequently affected electricity supply to natural gas and water infrastructure net-

†Corresponding author. E-mail: leinuo_zhang@zufe.edu.cn

© 2026 Chinese Physical Society and IOP Publishing Ltd. All rights, including for text and data mining, AI training, and similar technologies, are reserved.

works, exacerbating energy and water shortages.[13] Similarly, the Suez Canal cargo ship grounding incident in the same year highlighted the critical influence of logistics networks on overall supply chain networks.[14,15] These cases demonstrate that in highly interconnected modern infrastructure systems, single-network failures may propagate to multiple network systems through dependency relationships, causing systemic losses far exceeding localized impacts. Therefore, constructing theoretical models capable of characterizing such interdependency features is crucial for understanding and enhancing the resilience of infrastructure systems.

In research on the modeling of interdependent networks, classical models are primarily categorized into two types: node-coupled interdependent networks and edge-coupled interdependent networks. Buldyrev *et al.*[6] first proposed the node-coupled interdependent networks model in 2010, while Gao *et al.*[16] introduced the edge-coupled interdependent networks model in 2021, laying the theoretical foundation for subsequent research on load redistribution in interdependent networks.[17–20] Building upon these two models, scholars have conducted extensive research on load distribution mechanisms, proposing initial load setting methods based on topological features such as node degree and betweenness centrality[21–24] as well as nonlinear capacity models,[25] and applying these theoretical frameworks to real-world infrastructure systems including power–information interdependent networks,[21,26] transportation coupled networks,[18,27,28] and equipment support and command information systems.[22,23,25] Nevertheless, the single-type dependency relationships characterized by these classical models are insufficient to describe the more complex heterogeneous coupling patterns observed in real-world systems. To address this limitation, Gao *et al.*[29] proposed the binary interdependent network model in 2024, which couples nodes with edges, providing a novel theoretical framework for characterizing heterogeneous infrastructure systems.

Supply chain networks and logistics networks exhibit significant bidirectional dependency characteristics.[30] On the one hand, the normal operation of factory and warehousing nodes in supply chain systems heavily depends on transportation routes in logistics networks; on the other hand, the layout and operational efficiency of logistics routes are directly influenced by production planning, inventory strategies and order demands within supply chain systems. Given that both supply chain production capacities and logistics system transport capacities have upper limits, constructing a logistics–supply chain binary-coupled interdependent network model based on these dependency relationships and incorporating load redistribution mechanisms becomes an essential approach for understanding the robustness of such systems.

Based on the latest theoretical framework of binary interdependent networks, this study, for the first time, investigates the robustness of the logistics–supply chain binary-coupled network (LSBCN) model from the perspective of load redistribution. This research represents the first application and exploration of this theoretical framework in logistics–supply chain systems. It provides a novel analytical framework and perspective for system management, extending the current understanding of robustness in binary-coupled networks. The findings not only provide scientific decision-making support for enhancing national logistics hub resilience and optimizing strategies for supply chain risk prevention but also hold crucial practical value for ensuring smooth economic circulation in Xinjiang and achieving the dual objectives of "cost reduction and efficiency improvement" and "safety and controllability."

2. Logistics–supply chain interdependent networks model

2.1. Model development

In this study, edges serve as the primary functional elements of logistics networks, such as transportation routes and air routes. In contrast, the core functions of supply chain networks are assumed to be performed by nodes, such as factories, warehouses, and distribution centers. Therefore, a binary coupling model with edge-node dependence is adopted.[29] This paper constructs a basic theoretical model with structurally symmetric and fully interdependent edge-node coupling. In interdependent network research, such simplifications are commonly adopted to strip away the complex heterogeneity of real-world networks,[6,16,17,31,32] thereby more clearly revealing cascading failure and robustness patterns arising from interdependency, as shown in Fig. 1, where solid lines represent internal connections within a network while dashed lines denote interdependent edges between networks.

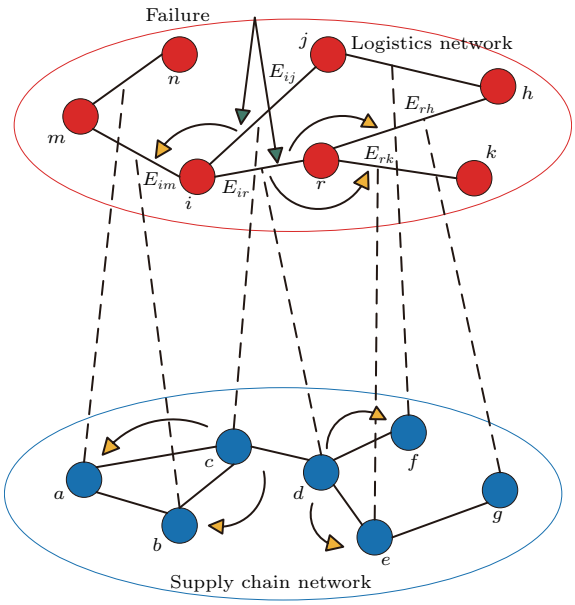


Fig. 1. Schematic diagram of the LSBCN model.

The loads of nodes and edges in the LSBCN are defined as follows:

$$L_c^A = k_c^{\alpha_1}, \tag{1}$$

$$L_{ij}^B = (k_i \times k_j)^{\alpha_2}, \tag{2}$$

where L_c^A and L_{ij}^B denote the initial load of node c in the supply chain network and the E_{ij} edge in the logistics network, respectively. α_1 and α_2 are adjustable parameters, k_c denotes the degree of node c in the supply chain network, and k_i and k_j denote the degrees of nodes i and j in the logistics network. In the supply chain network, a higher node degree indicates a greater load that must be handled. Defining the initial load of nodes and edges as a linear relationship with degree is a common setting in interdependent network load research.[18,19,24,28,33,34] In this study, the larger the degree of a node in the supply chain network, the more load the node needs to handle; in the logistics network, the transportation volume of routes connecting two hub nodes is certainly greater than that of routes connecting two ordinary nodes. Therefore, we consider the initial load of nodes and edges to also have a linear relationship with degree, and thus set $\alpha_1 = \alpha_2 = 1$.

Since the nonlinear relationship between load and capacity for nodes and edges better aligns with real-world networks,[25] this paper adopts a nonlinear load-capacity model. Therefore, the initial capacities for nodes and edges in the network are as follows:

$$C_c^A = L_c^A + (\beta_1 L_c^A)^{\gamma_1}, \tag{3}$$

$$C_{ij}^B = L_{ij}^B + (\beta_2 L_{ij}^B)^{\gamma_2}, \tag{4}$$

where β_1 and β_2 are variable load capacity factors, while γ_1 and γ_2 are variable load capacity indices. If node c in the supply chain network fails, its adjacent nodes will receive the load ΔL_c^A. Similarly, the load will be redistributed among its adjacent edges according to a specific distribution fraction if edge E_{ij} in the logistics network fails. At this point, the load of node b adjacent to node c in the supply chain network and the load of edge E_{im} adjacent to E_{ij} in the logistics network are

$$\begin{cases} L_b^{A'} = L_b^A + \Delta L_c^A \\ L_{im}^{B'} = L_{im}^B + \Delta L_{im}^B. \end{cases} \tag{5}$$

When $L_b^{A'} > C_b^A$, node b becomes overloaded and fails; then, the load from the failed node is redistributed to its adjacent nodes. Similarly, when $L_{im}^{B'} > C_{im}^B$, edge E_{im} becomes overloaded and fails, and the load from the failed edge is redistributed to its adjacent edges.

2.2. Dynamic load distribution strategy

To better analyze the robustness of an LSBCN, this paper proposes a dynamic residual capacity load distribution strategy. The distribution fraction is dynamically adjusted based on the real-time residual capacity of adjacent nodes or edges, as illustrated in Fig. 2.

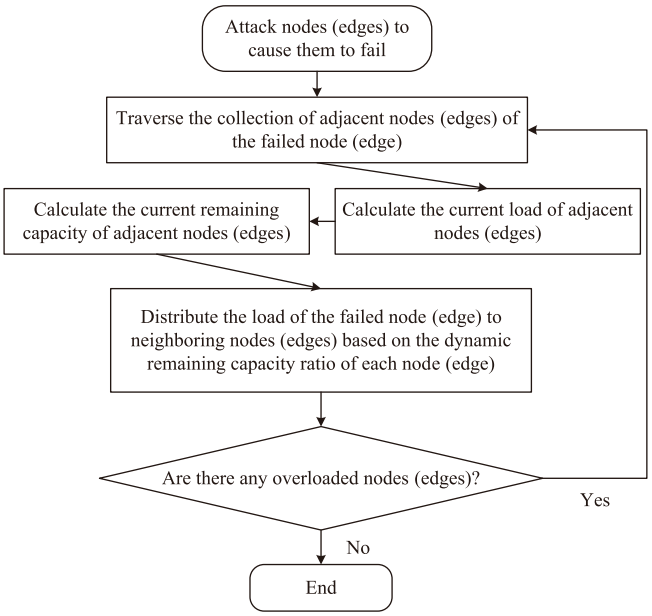


Fig. 2. Flowchart of the dynamic residual capacity load distribution algorithm.

When edge E_{ij} fails, the expression for the dynamic residual capacity load distribution strategy is

$$\Delta L_{ij}^B = L_{ij}^B \times \frac{C_{im}^B - \tilde{L}_{im}^B}{\sum\limits_{x\in\Gamma_i}\left(C_{ix}^B - \tilde{L}_{ix}^B\right) + \sum\limits_{y\in\Gamma_j}\left(C_{jy}^B - \tilde{L}_{jy}^B\right)}, \tag{6}$$

where C_{im}^B and $\tilde{L}_{im}^B$ denote the capacity and prior distribution load of the adjacent edge E_{im}, respectively. Γ_i and Γ_j represent the collection of neighbors for nodes i and j, respectively.

When node c fails, the expression for the dynamic residual capacity load distribution strategy is

$$\Delta L_b^A = L_c^A \times \frac{C_b^A - \tilde{L}_b^A}{\sum_{x\in\Gamma_c}\left(C_x^A - \tilde{L}_x^A\right)}, \tag{7}$$

where C_b^A denotes the capacity of the adjacent node b, $\tilde{L}_b^A$ represents the load of the adjacent node b prior to the load distribution process, and Γ_c denotes the collection of nodes adjacent to node c.

Under this dynamic distribution strategy, nodes (edges) with greater remaining capacity absorb a larger share of the load from failed nodes (edges).

2.3. Cascade failure process and robustness evaluation metric

The failure mechanisms considered in this study comprise three types: overload failure, dependency failure, and connectivity failure. These mechanisms operate as follows: (1) in overload failure a supply chain node or logistics edge fails when its load exceeds its designated capacity; (2) in dependency failure a supply chain node fails when all its dependent logistics edges fail, whereas a logistics edge fails when its dependent supply chain node fails; and (3) in connectivity failure

a node or edge fails upon disconnection from the giant component (GC).[6,16]

Figure 3 illustrates the cascading failure process in a LSBCN. As depicted in Fig. 3(a), when edges E_{ij} and E_{ir} in the logistics network fail, their loads are redistributed to neighboring edges E_{im}, E_{rh}, and E_{rk}. Simultaneously, the dependent supplier nodes c and d in the supply chain network also fail, redistributing their loads to neighboring nodes a, b, e, and f. Suppose that node a subsequently fails due to overload and node b fails due to disconnection from the GC; this triggers the failure of logistics edges dependent on these nodes. Although edges E_{rh} and E_{rk} and nodes e and f receive additional loads, these remain within their respective capacity limits, preventing further overload failures. The network thus reaches a stable state, as shown in Fig. 3(b).

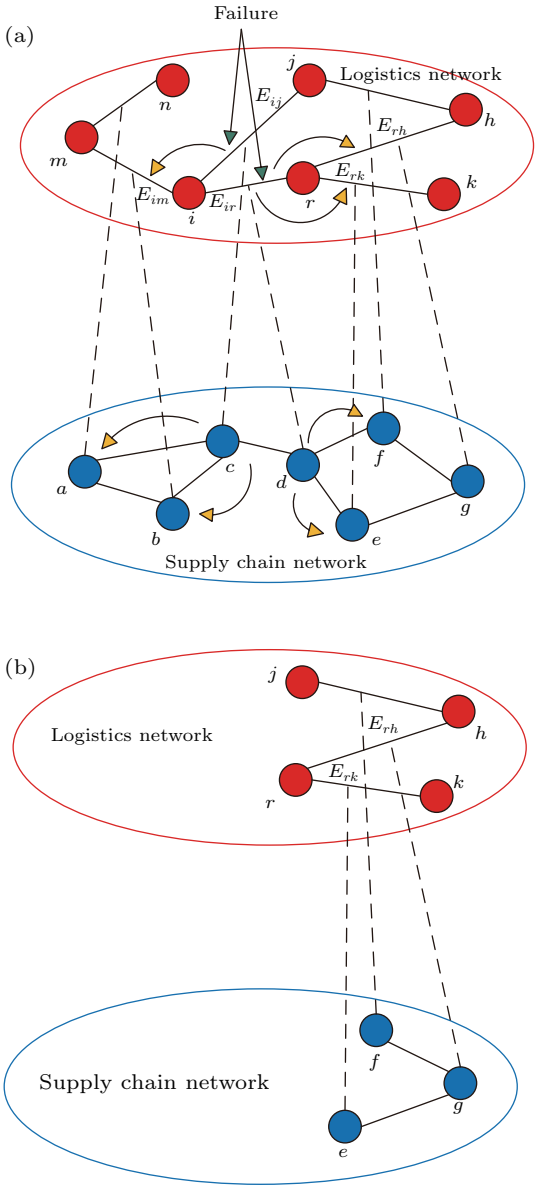


Fig. 3. Cascading failure of a LSBCN.

The integrity of the network topology following cascading failures is closely linked to the fragility of the network. The more complete the remaining topology, the faster the network recovers from a failed state. Let p denote the fraction of the initial number of nodes (edges) that remain after a failure. The surviving scale F represents the topological integrity of the network after a failure,

$$\begin{cases} F_{\mathrm{G}} = \dfrac{\tilde{N}_A}{N_A}, \\ F_{\mathrm{W}} = \dfrac{\tilde{E}_B}{E_B}. \end{cases} \tag{8}$$

Here F_{G} and F_{W} denote the survival scales of the supply chain network and the logistics network, respectively. $\tilde{N}_A$ and $\tilde{E}_B$ represent the number of remaining nodes and edges in the supply chain network and the logistics network, respectively, after cascading failures. N_A and E_B denote the number of nodes and edges in the supply chain network and the logistics network, respectively, before cascading failures. A larger F value indicates less network damage, signifying better network robustness.

3. Simulation analysis

3.1. Robustness analysis of networks under different failure conditions

In the real world, supply chain networks and logistics networks exhibit significant scale-free characteristics. Research indicates that the average degree of most logistics networks ranges from two to three, while supply chain networks typically have an average degree of around eight.[35–39] Therefore, this study models both logistics and supply chain networks as BA scale-free networks. The logistics network has 2000 nodes and an average degree of three, while the supply chain network comprises 3000 nodes with an average degree of eight. Failure modes involve the random or deliberate failure of a fraction $1-p$ of edges (nodes) in the network. Deliberate failures prioritize edges with higher failure indices and nodes with higher degrees. Capacity factors $\beta_1 = \beta_2 = 1$ and capacity indices $\gamma_1 = \gamma_2 = 1$ are adopted, with 100 simulation runs conducted. Simulation results are presented in Fig. 4.

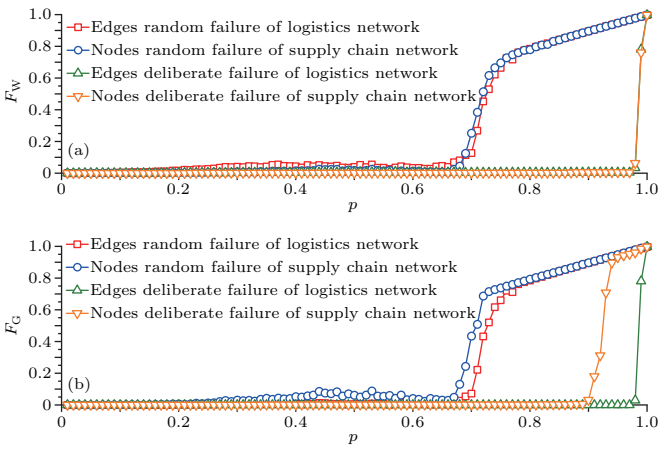


Fig. 4. Plot of F_{W} and F_{G} with p during random and deliberate failures.

Table 1. The critical threshold p_c for complete LSBCN collapse.

Curve type	Edges random failure of logistics network	Nodes random failure of supply chain network	Edges deliberate failure of logistics network	Nodes deliberate failure of supply chain network
p_c (F_W)	0.71	0.7	0.98	0.98
p_c (F_G)	0.71	0.69	0.98	0.92

To quantitatively identify the critical threshold at which a complete LSBCN collapse occurs, we calculated the first-order derivative $\mathrm{d}F/\mathrm{d}p$ for each curve in Fig. 4. As p gradually decreases from 1, when $\mathrm{d}F/\mathrm{d}p$ suddenly drops from its peak to a smaller value, it indicates that a large-scale collapse has occurred in the system. The p value corresponding to this peak is defined as the critical collapse threshold p_c, representing the critical point of a complete system collapse. The calculated p_c values are summarized in Table 1.

From Fig. 4 and Table 1, it can be observed that the logistics–supply chain network requires approximately 30% ($p_c \approx 0.7$) of nodes or edges to fail under random failure to completely collapse, whereas under deliberate failure a failure ratio of only about 2% ($p_c \approx 0.98$) can cause sharp declines in F_W and F_G. This indicates that, due to heterogeneity in betweenness and degree distributions within logistics supply chain networks, most edges exhibit low betweenness or nodes have low degrees. Random failures primarily affect non-core edges or nodes, to which the network exhibits relatively strong robustness. In contrast, deliberate failures target critical edges and hub nodes, rapidly disrupting network connectivity.

Supply chain networks exhibit higher average degrees than logistics networks. When subjected to both random and deliberate failures, supply chain networks exhibit slightly greater robustness than logistics networks from the perspective of F_G. However, they still experience abrupt collapse under deliberate failure scenarios. This indicates that network density has a minor impact on robustness, with critical edges and nodes remaining the key determinants.

3.2. Robustness analysis under variation of capacity factors

We investigate how the robustness of LSBCN evolves with varying capacity factors. Both capacity factors β_1 and β_2 are defined in the range [0, 2] while the capacity indices γ_1 and γ_2 are set to 1. The fraction p of retained edges (or nodes) during random failures is set to 0.6, 0.7, and 0.8, respectively. Other network structural parameters remain consistent with those in the preceding section. The simulation results for varying β_1 are shown in Fig. 5.

To quantitatively evaluate the impact of β_1 on network robustness, we adopted the total improvement magnitude $\Delta F_{\beta_1} = \max(F) - \min(F)$ to assess the effectiveness of β_1. The larger the total improvement magnitude, the more significant the variation of F and β_1, indicating that adjusting β_1 is more effective for enhancing robustness. The ΔF_{β_1} values for all curves in Fig. 5 are provided in Table 2.

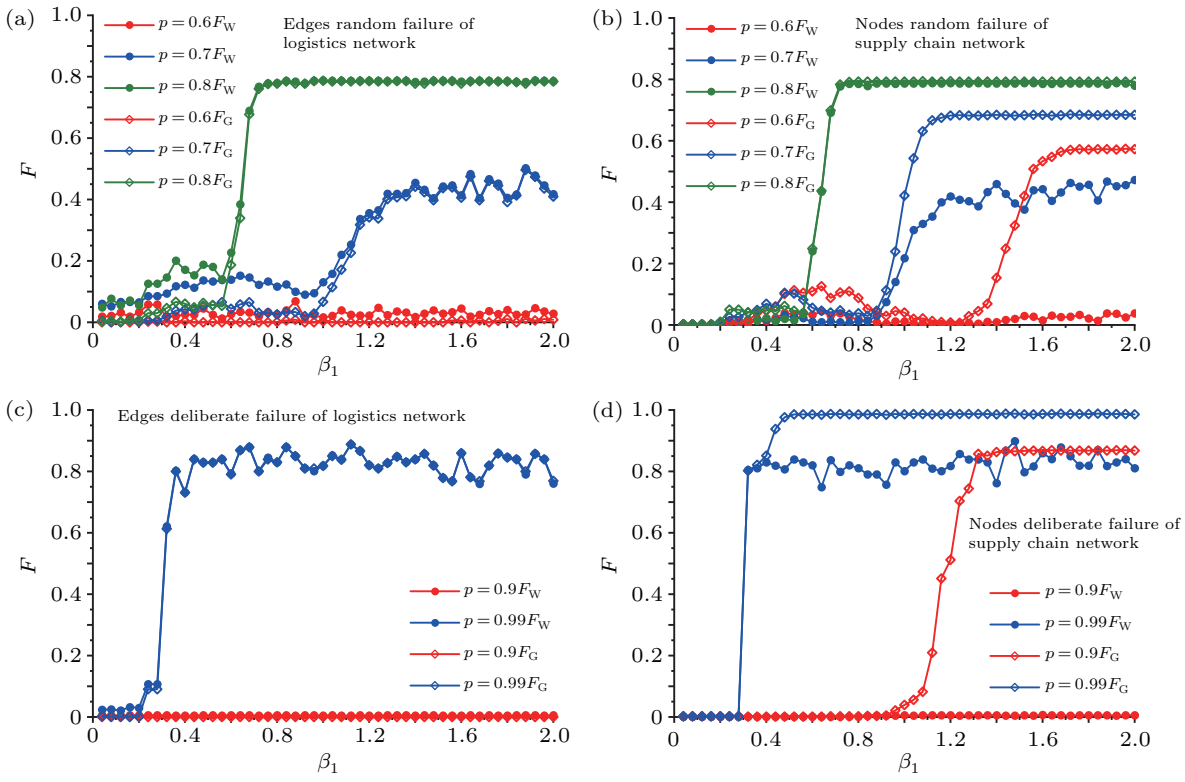


Fig. 5. Plot of capacity factor β_1 and survival scale F.

Table 2. The ΔF_{β_1} values of the curves in Fig. 5.

	Fig. 5(a)	Fig. 5(a)	Fig. 5(b)	Fig. 5(b)		Fig. 5(c)	Fig. 5(c)	Fig. 5(d)	Fig. 5(d)
	F_W	F_G	F_W	F_G		F_W	F_G	F_W	F_G
$p=0.6$	0.06	0.01	0.04	0.57	$p=0.9$	0.002	0	0.007	0.87
$p=0.7$	0.45	0.50	0.47	0.68	$p=0.99$	0.87	0.89	0.90	0.99
$p=0.8$	0.74	0.78	0.79	0.79					

Table 3. The β_{1c} values of the curves in Fig. 5.

	Fig. 5(a)	Fig. 5(a)	Fig. 5(b)	Fig. 5(b)		Fig. 5(c)	Fig. 5(c)	Fig. 5(d)	Fig. 5(d)
	F_W	F_G	F_W	F_G		F_W	F_G	F_W	F_G
$p=0.6$	–	–	–	1.60	$p=0.9$	–	–	–	1.36
$p=0.7$	1.32	1.32	1.28	1.16	$p=0.99$	0.36	0.36	0.36	0.48
$p=0.8$	0.76	0.76	0.72	0.72					

Table 4. The ΔF_{β_2} values of the curves in Fig. 6.

	Fig. 6(a)	Fig. 6(a)	Fig. 6(b)	Fig. 6(b)		Fig. 6(c)	Fig. 6(c)	Fig. 6(d)	Fig. 6(d)
	F_W	F_G	F_W	F_G		F_W	F_G	F_W	F_G
$p=0.6$	0.37	0.07	0.01	0.06	$p=0.9$	0.007	0	0.006	0.006
$p=0.7$	0.53	0.35	0.47	0.17	$p=0.99$	0.99	0.99	0.99	0.02
$p=0.8$	0.79	0.79	0.79	0.02					

Table 5. The β_{2c} values of the curves in Fig. 6.

	Fig. 6(a)	Fig. 6(a)	Fig. 6(b)	Fig. 6(b)		Fig. 6(c)	Fig. 6(c)	Fig. 6(d)	Fig. 6(d)
	F_W	F_G	F_W	F_G		F_W	F_G	F_W	F_G
$p=0.6$	2	–	–	–	$p=0.9$	–	–	–	–
$p=0.7$	2	2	1.08	–	$p=0.99$	1.16	1.16	1.2	–
$p=0.8$	0.88	0.88	0.84	–					

Based on the data in Table 2, when $\Delta F_{\beta_1} > 0.4$ increasing β_1 is considered to significantly enhance network robustness. Accordingly, when the logistics network fails, increasing β_1 is effective for $p = 0.7$, 0.8 and 0.99 (i.e., when the failure ratio is approximately equal to or below the critical value of complete network collapse), but not effective for $p = 0.6$ and 0.9 (i.e., when the failure ratio exceeds the critical value of complete network collapse). When the supply chain network fails, except for a few cases, increasing β_1 generally improves robustness.

Furthermore, when β_1 increases from 0 to 2, we calculate the value of $\mathrm{d}F/\mathrm{d}\beta_1$. If it exhibits an evolutionary characteristic of low value $\rightarrow$ peak value $\rightarrow$ low value, it indicates that the robustness of the system has been significantly improved within this interval. We define the critical capacity parameter β_{1c} as the β_1 value when $\mathrm{d}F/\mathrm{d}\beta_1$ falls back to near 0 after the peak, at which point continuing to increase β_1 has a limited effect on robustness improvement. The β_{1c} values for curves with significant changes in Fig. 5 are provided in Table 3.

The analysis results show that increasing β_1 has significant effects on random failure ($p = 0.7$, 0.8) and deliberate failure ($p = 0.99$) scenarios for the logistics network, with optimal thresholds of $\beta_1 \geq 1.32$, $\beta_1 \geq 0.76$, and $\beta_1 \geq 0.36$, respectively. For the supply chain network, the optimal thresholds for random failure scenarios at $p = 0.6$, 0.7, and 0.8 are $\beta_1 \geq 1.60$, $\beta_1 \geq 1.28$, and $\beta_1 \geq 0.72$, respectively; for deliberate failure scenarios at $p = 0.9$ and $p = 0.99$ the optimal thresholds are $\beta_1 \geq 1.36$ and $\beta_1 \geq 0.48$, respectively.

Figure 6 shows the simulation results when β_2 varies. Similarly, we adopt the total improvement magnitude ΔF_{β_2} to evaluate the effectiveness of β_2. Table 4 presents the ΔF_{β_2} values for all curves in Fig. 6.

When $\Delta F_{\beta_2} > 0.3$, increasing β_2 is considered to significantly enhance network robustness. Accordingly, when the logistics network fails, increasing β_2 is effective for $p = 0.7$, 0.8, and 0.99; at $p = 0.6$, increasing β_2 has only a certain effect on the logistics network. When the supply chain network fails, increasing β_2 is effective only for the logistics network at $p = 0.7$, 0.8, and 0.99.

Furthermore, we calculate $\mathrm{d}F/\mathrm{d}\beta_2$ when β_2 ranges from 0 to 2 and obtain the critical capacity parameter β_{2c}. Table 5 presents the β_{2c} values for curves with significant changes in Fig. 6.

In summary, the optimal thresholds for β_2 are: for random failure of the logistics network ($p = 0.8$), $\beta_2 \geq 0.88$; and for deliberate failure ($p = 0.99$), $\beta_2 \geq 1.16$. For a supply chain network under random failure ($p = 0.7$, 0.8), the optimal thresholds are $\beta_2 \geq 1.08$ and $\beta_2 \geq 0.84$, respectively; for deliberate failure ($p = 0.99$), $\beta_2 \geq 1.20$.

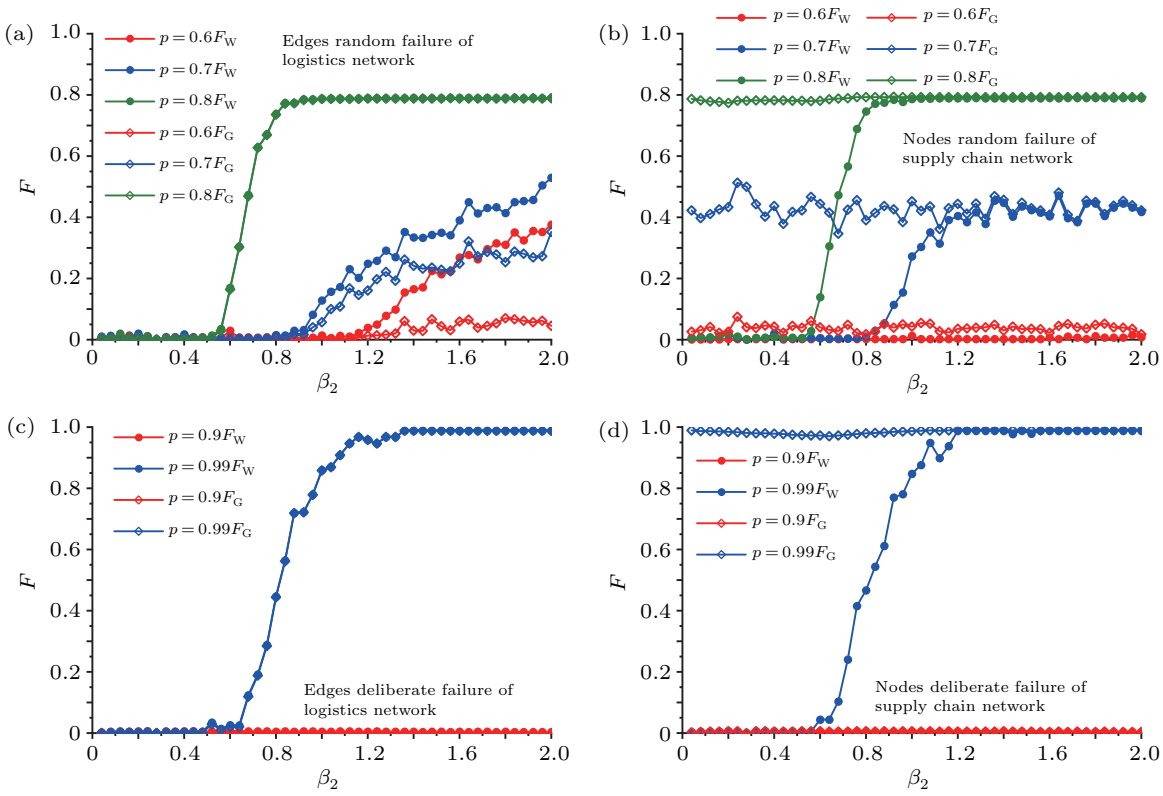


Fig. 6. Plot of capacity factor β_2 and survival scale F.

3.3. Robustness analysis under capacity index variation

To investigate how the robustness of a LSBCN evolves with varying capacity indices, both γ_1 and γ_2 were sampled from [0, 2] while the capacity factors β_1 and β_2 were set to 1. The fraction p of retained edges (nodes) during random failures was set to 0.6, 0.7, and 0.8, respectively. Other network structural parameters remained consistent with the previous section. Simulation results for varying γ_1 are shown in Fig. 7.

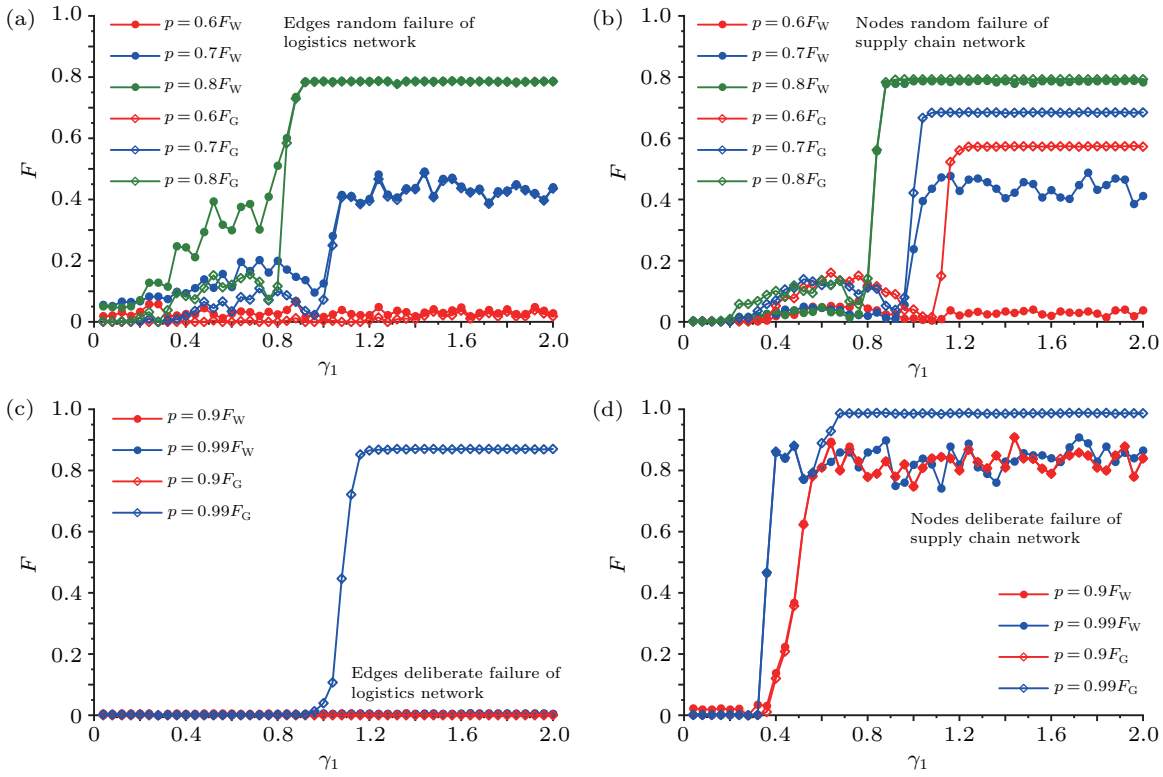


Fig. 7. Plot of capacity index γ_1 and survival scale F.

Table 6. The ΔF_{γ_1} values of the curves in Fig. 7.

	Fig. 7(a)	Fig. 7(a)	Fig. 7(b)	Fig. 7(b)		Fig. 7(c)	Fig. 7(c)	Fig. 7(d)	Fig. 7(d)
	F_W	F_G	F_W	F_G		F_W	F_G	F_W	F_G
$p=0.6$	0.06	0.04	0.07	0.57	$p=0.9$	0.007	0	0.91	0.91
$p=0.7$	0.44	0.49	0.49	0.68	$p=0.99$	0.007	0.87	0.91	0.99
$p=0.8$	0.74	0.79	0.79	0.79					

Table 7. The γ_{1c} values of the curves in Fig. 7.

	Fig. 7(a)	Fig. 7(a)	Fig. 7(b)	Fig. 7(b)		Fig. 7(c)	Fig. 7(c)	Fig. 7(d)	Fig. 7(d)
	F_W	F_G	F_W	F_G		F_W	F_G	F_W	F_G
$p=0.6$	–	–	–	1.24	$p=0.9$	–	–	0.64	0.64
$p=0.7$	1.12	1.12	1.12	1.08	$p=0.99$	–	1.2	0.44	0.68
$p=0.8$	0.96	0.96	0.92	0.92					

Table 8. The ΔF_{γ_2} values of the curves in Fig. 8.

	Fig. 8(a)	Fig. 8(a)	Fig. 8(b)	Fig. 8(b)		Fig. 8(c)	Fig. 8(c)	Fig. 8(d)	Fig. 8(d)
	F_W	F_G	F_W	F_G		F_W	F_G	F_W	F_G
$p=0.6$	0.52	0.09	0.05	0.05	$p=0.9$	0.88	0.30	0.84	0.24
$p=0.7$	0.66	0.38	0.47	0.12	$p=0.99$	0.99	0.99	0.99	0.02
$p=0.8$	0.79	0.79	0.79	0.02					

Table 9. The γ_{2c} values of the curves in Fig. 8.

	Fig. 8(a)	Fig. 8(a)	Fig. 8(b)	Fig. 8(b)		Fig. 8(c)	Fig. 8(c)	Fig. 8(d)	Fig. 8(d)
	F_W	F_G	F_W	F_G		F_W	F_G	F_W	F_G
$p=0.6$	1.32	–	–	–	$p=0.9$	1.4	1.48	1.4	1.4
$p=0.7$	1.32	1.12	1.12	–	$p=0.99$	1.08	1.08	1.04	–
$p=0.8$	1	1	1	–					

Similarly, we adopt the total improvement magnitude ΔF_{γ_1} to quantitatively evaluate the impact of γ_1 on network robustness. Table 6 presents the ΔF_{γ_1} values for all curves in Fig. 7.

When $\Delta F_{\gamma_1} > 0.4$, increasing γ_1 is considered to significantly enhance network robustness. Accordingly, when the logistics network fails, increasing γ_1 is effective at $p = 0.7$ and 0.8; at $p = 0.99$, increasing γ_1 is only effective for the supply chain network. When the supply chain network fails, increasing γ_1 is only effective for the supply chain network at $p = 0.6$; in all other cases, increasing γ_1 is effective.

Furthermore, we calculate $\mathrm{d}F/\mathrm{d}\gamma_1$ when γ_1 ranges from 0 to 2 and obtain the critical capacity parameter γ_{1c}. Table 7 presents the γ_{1c} values for curves with significant changes in Fig. 7.

The analysis results show that for random failure of the logistics network, the optimal thresholds are $\gamma_1 \geq 1.12$ at $p = 0.7$ and $\gamma_1 \geq 0.96$ at $p = 0.8$; for deliberate failure ($p = 0.99$), $\gamma_1 \geq 1.20$. For a supply chain network under random failure, the optimal thresholds at $p = 0.6$, 0.7, and 0.8 are $\gamma_1 \geq 1.24$, $\gamma_1 \geq 1.12$, and $\gamma_1 \geq 0.92$, respectively; for deliberate failure at $p = 0.9$ and $p = 0.99$, the optimal thresholds are $\gamma_1 \geq 0.64$ and $\gamma_1 \geq 0.68$, respectively.

Figure 8 shows the simulation results when γ_2 varies. Similarly, we adopt the total improvement magnitude ΔF_{γ_2} to quantitatively evaluate the impact of γ_2 on network robustness. Table 8 presents the ΔF_{γ_2} values for all curves in Fig. 8.

When $\Delta F_{\gamma_2} \geq 0.2$, increasing γ_2 is considered to significantly enhance network robustness. Accordingly, when the logistics network fails, increasing γ_2 is only effective for the logistics network at $p = 0.6$; in all other cases, increasing γ_2 is effective. When the supply chain network fails, increasing γ_2 is only effective for the logistics network at $p = 0.7$, 0.8, 0.9, and 0.99.

Furthermore, we calculate $\mathrm{d}F/\mathrm{d}\gamma_2$ when γ_2 ranges from 0 to 2 and obtain the critical capacity parameter γ_{2c}. Table 9 presents the γ_{2c} values for curves with significant changes in Fig. 8.

In summary, the optimal thresholds for γ_2 are as follows: for random failure of the logistics network, the optimal thresholds are $\gamma_2 \geq 1.32$ at $p = 0.6$ and $p = 0.7$, and $\gamma_2 \geq 1.00$ at $p = 0.8$; for deliberate failure at $p = 0.9$ and $p = 0.99$, the optimal thresholds are $\gamma_2 \geq 1.48$ and $\gamma_2 \geq 1.08$, respectively. For a supply chain network under random failure ($p = 0.7$, 0.8), the optimal thresholds for logistics network robustness are $\gamma_2 \geq 1.12$ and $\gamma_2 \geq 1.00$, respectively; for deliberate failure at $p = 0.9$ and $p = 0.99$, the optimal thresholds are $\gamma_2 \geq 1.40$ and $\gamma_2 \geq 1.04$, respectively.

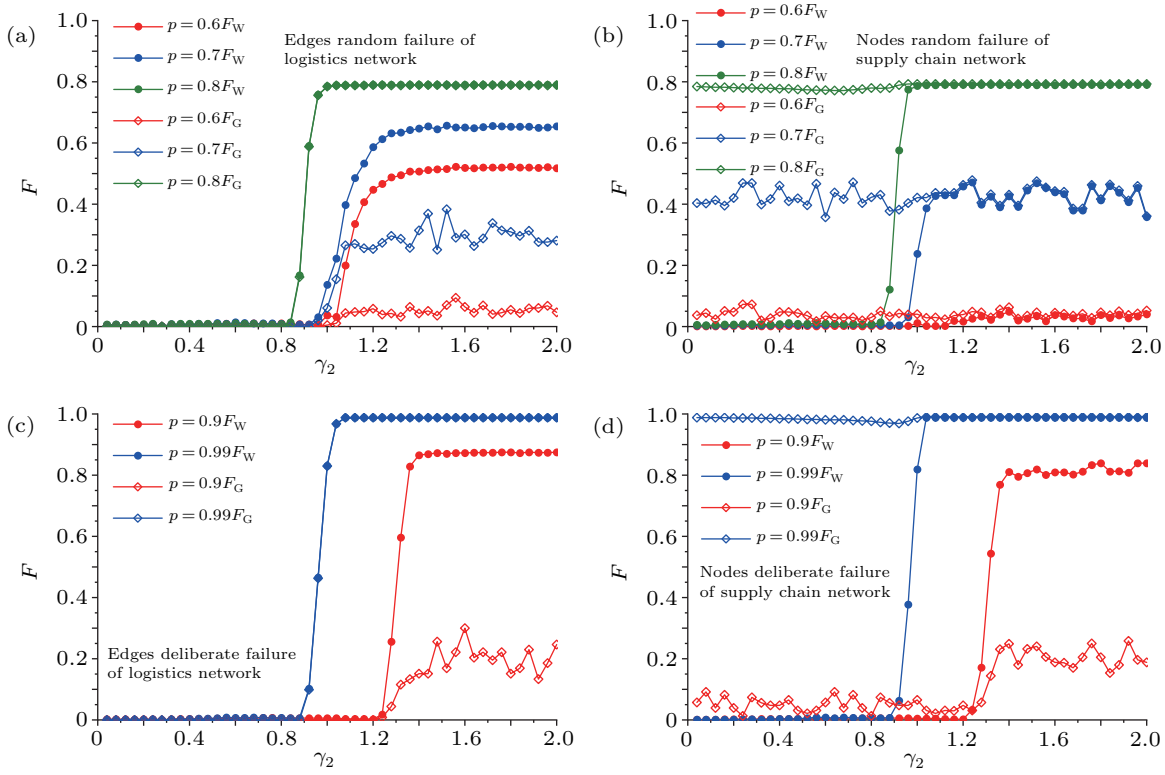


Fig. 8. Plot of capacity index γ_2 and survival scale F.

Furthermore, the above analysis reveals that in certain scenarios, when the failure fraction exceeds the critical threshold for complete network collapse, increasing the capacity parameters becomes ineffective for improving network robustness. For instance, at $p = 0.6$ and $p = 0.9$, enhancing β_1 and β_2 shows no improvement in the robustness of the logistics network. The explanation for this phenomenon is as follows.

(1) From the perspective of network structure, when the failure ratio p exceeds the critical threshold p_c, the GC in the network splits into isolated small components. This structural collapse is the primary reason why capacity parameters become ineffective. The GC, which carries most of the network traffic, fragments into disconnected small components. Without a connected network structure, regardless of how much capacity individual nodes or edges possess, loads cannot be transmitted between different parts of the network.

(2) From the perspective of the load redistribution mechanism, the load redistribution mechanism in this model fundamentally relies on surviving neighboring nodes or edges to share the additional load from failed components. When $p > p_c$, as the GC splits and fragments, the number of available neighbor nodes or edges for redistribution drops sharply. These surviving neighbors must not only absorb their original loads but also absorb the redistributed loads from failed components. Their load growth rate exceeds what the capacity can accommodate, causing them to transfer accumulated loads to fewer surviving nodes or edges and thereby accelerating the collapse of the entire network.

Therefore, when $p > p_c$, the interaction between the network structure and the load redistribution mechanism causes increases in the capacity parameter to become ineffective. The splitting of the GC structurally eliminates most redistribution paths, while the load redistribution mechanism can cause further structural damage through cascading failures.

4. Robust optimization strategy

4.1. Optimize the network's capacity parameters

Based on the analysis of different capacity factors and capacity indices in Subsection 3.2, the network's robustness improves continuously as β and γ increase, regardless of whether failures are random or deliberate. Starting from a baseline where both β and γ are set to 1, we increased the magnitudes of the capacity parameters. We conducted computer simulations of logistics–supply chain networks under different capacity parameter configurations. The resulting relationship between F and p is illustrated in Fig. 9.

As shown in Fig. 9, increasing the capacity parameter significantly enhances network robustness. When the fraction of random failures exceeds approximately 25%, increasing the capacity parameter gradually improves network robustness. For deliberate failures, capacity parameters β and γ at 1.1 yield negligible robustness enhancement; robustness only improves when β and γ exceed 1.3. Simultaneously optimizing the capacity parameters yields greater improvements in robustness for logistics networks than for supply chain networks.

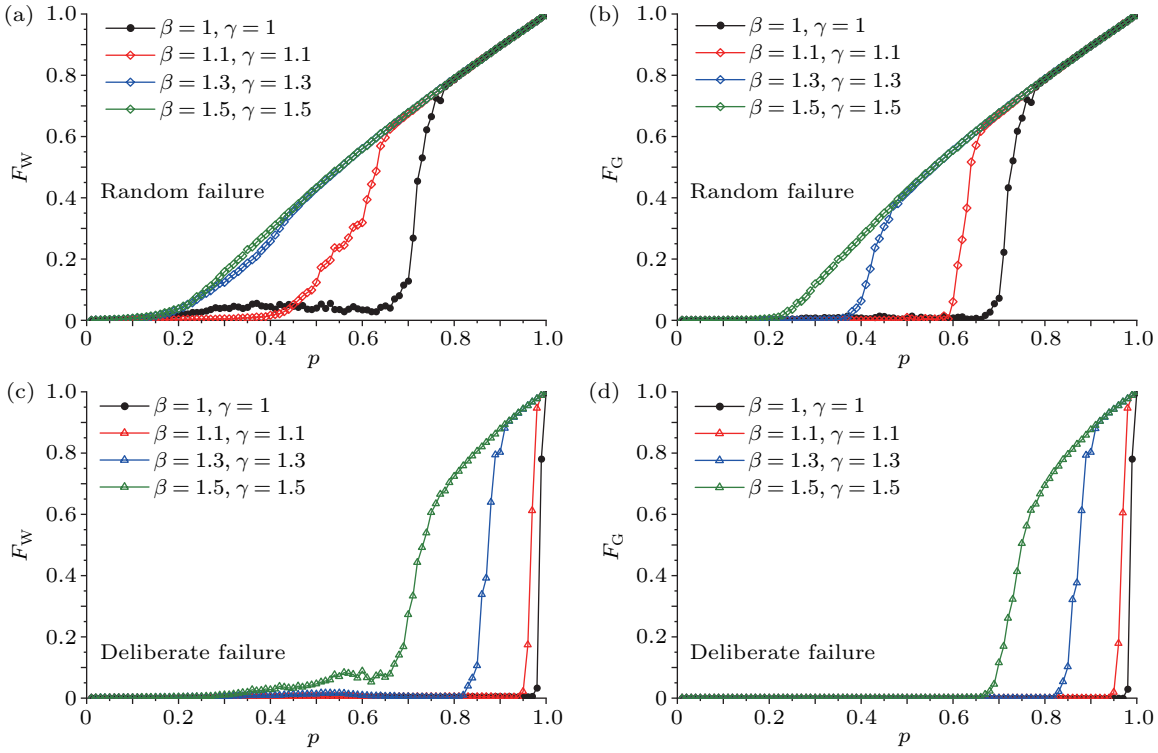


Fig. 9. Plot of F and p after optimizing capacity parameters.

To further seek the optimal combination of capacity parameters, the capacity parameter optimization is formulated as an unconstrained nonlinear optimization problem. The objective function is defined as follows:

$$\max_{\beta,\gamma} F(\beta_1, \gamma_1, \beta_2, \gamma_2), \tag{9}$$

where F represents the average of F_W and F_G, i.e., $F = \frac{1}{2}(F_W + F_G)$. The constraints are $\beta, \gamma \in (0, 2]$. Since the objective function $F(\cdot)$ is an implicit function that must be evaluated through Monte Carlo simulations, a genetic algorithm is employed to identify the optimal capacity parameters under different failure types and proportions. Subsequently, the values of F under both the optimal capacity parameters and the maximum capacity parameters are computed, denoted as $F_{\max}$ and $F_{\beta=\gamma=2}$, respectively. The results are presented in Table 10.

Table 10. Optimal capacity parameters under failures.

Failure mode	p	β_1	β_2	γ_1	γ_2	$F_{\max}$	$F_{\beta=\gamma=2}$
Random failure	0.6	1.63	1.47	1.48	1.58	0.557	0.557
Random failure	0.7	1.12	1.41	1.75	1.60	0.677	0.678
Random failure	0.8	0.86	1.05	1.39	1.53	0.789	0.789
Deliberate failure	0.9	0.70	1.34	1.88	1.59	0.878	0.879
Deliberate failure	0.99	1.34	0.80	1.48	1.41	0.988	0.988

As shown in Table 10, the optimal capacity parameter configurations vary across different failure scenarios. Notably, the maximum robustness achieved under optimal capacity parameters ($F_{\max}$) is almost identical to that under maximum capacity parameters ($F_{\beta=\gamma=2}$). This finding indicates that parameter optimization enables comparable robustness enhancement without necessitating the maximization of all parameters.

4.2. Critical edge protection

Protecting critical edges in a logistics network can also enhance its robustness. By ranking edges based on betweenness and protecting the top s_p% of them, overload failures can be prevented. Figure 10 illustrates the relationship between F and p for different s_p values under random and deliberate failures.

As shown in Fig. 10, protecting critical edges in logistics networks during random failures can enhance network robustness to a certain extent, with better protective effects observed in logistics networks than in supply chain networks. However, during deliberate failures, protecting critical edges in logistics networks does not significantly improve network robustness, yielding only a very slight improvement when $s_p = 10\%$.

4.3. Add redundant edges

In addition to protecting critical edges in the logistics network, redundant edges can be established for these critical edges. This ensures that when one edge fails, an alternative edge remains available. Similarly, edges are sorted by their betweenness, and redundant edges are configured for the top s_r% of sorted edges. Under random and deliberate failure conditions, the relationship between F and p for different s_r values is illustrated in Fig. 11.

As shown in Fig. 11, adding redundant edges to the logistics network does not significantly enhance its robustness during random failures. However, during deliberate failures, introducing redundant edges significantly improves the network's robustness, with a greater effect observed in logistics networks than in supply chain networks.

By combining these three robustness optimization strategies, protecting critical edges in logistics networks can significantly enhance network robustness during random failures. Adding redundant edges to logistics networks significantly improves robustness during deliberate failures, and optimizing network capacity parameters enhances robustness across all failure conditions.

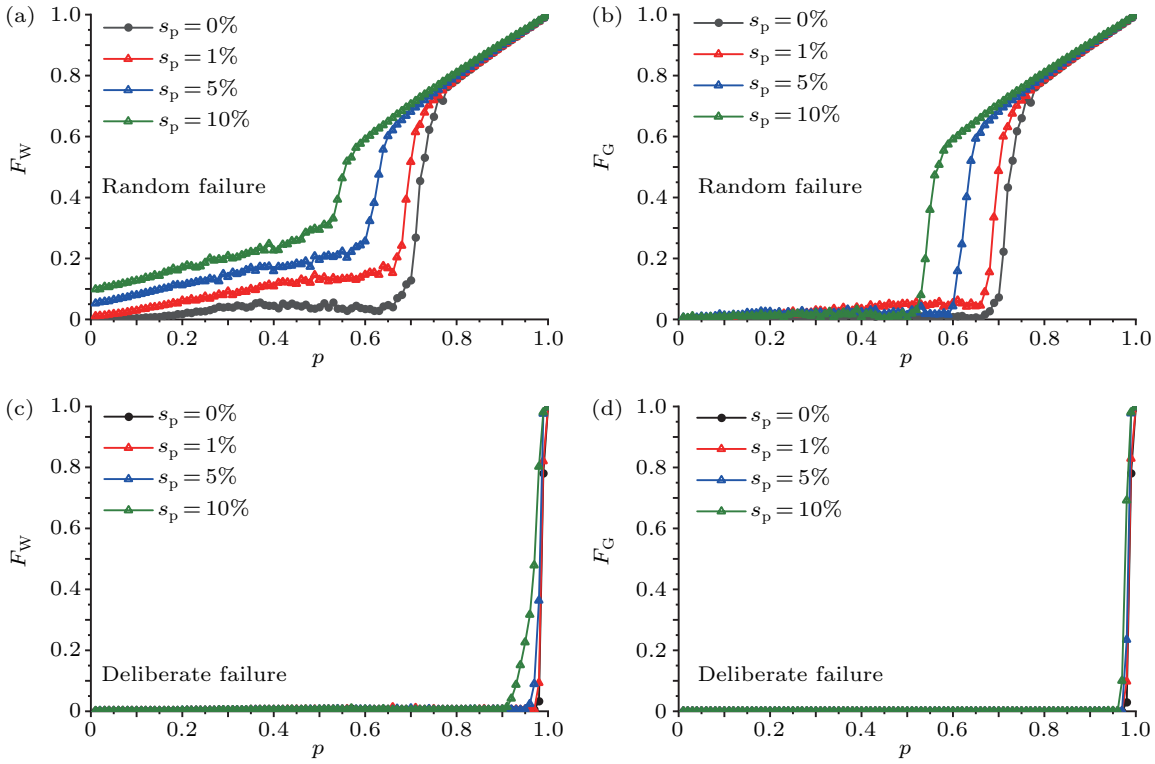


Fig. 10. Plot of F and p under the critical edge protection strategy.

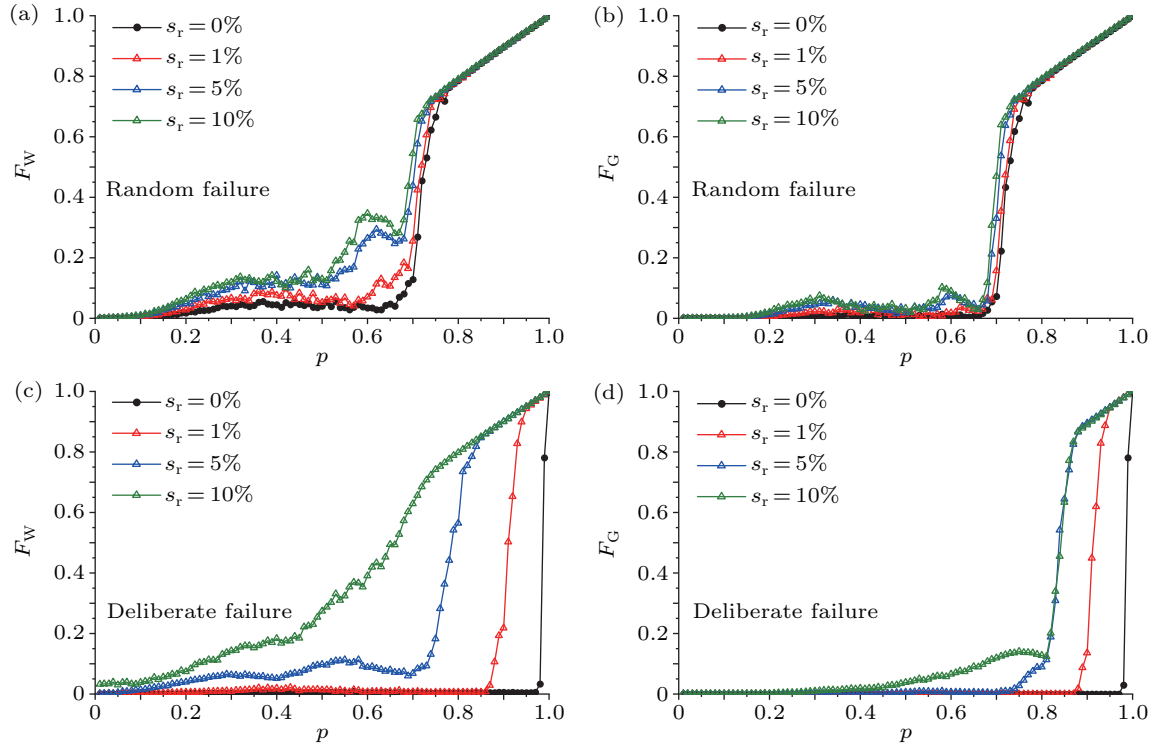


Fig. 11. Plot of F and p under the redundant edge addition strategies.

5. Discussion

5.1. Synergistic effect analysis

To evaluate the synergistic effects of the three strategies, we designed strategy combination experiments using the control variable method to assess the effects of pairwise combinations and the simultaneous implementation of all three strategies. Let the three strategies be as follows: S_1, optimize capacity parameters; S_2, protect critical edges; S_3, add redundant edges. We define the synergistic effect factor, η, to quantify the synergistic effects of strategy combinations:

$$\eta = \frac{F_{S_i+S_j} - F_{\text{base}}}{(F_{S_i} - F_{\text{base}}) + (F_{S_j} - F_{\text{base}})} - 1, \tag{10}$$

where F_{base} is the baseline robustness, F_{S_i} is the robustness when using strategy S_i alone, and $F_{S_i+S_j}$ is the robustness under the combined strategy. If $\eta > 0$, it indicates positive synergistic effects between different strategies; if $\eta = 0$, it indicates that strategy effects are independent; if $\eta < 0$, it indicates negative synergistic effects between strategies.

Let the optimization parameters for S_1 be $\beta = \gamma = 1.1$, for S_2 be $s_{\text{p}} = 1\%$, and for S_3 be $s_{\text{r}} = 1\%$. Computer simulations were conducted under random failure ($p = 0.6$, 0.7, 0.8) and deliberate failure ($p = 0.9$, 0.99) scenarios. The simulation results are shown in Table 11.

From these results, it can be concluded that the effects of strategy combinations are not simply additive but exhibit complex synergistic effects, as detailed below.

Under random failure, at higher failure ratios ($p = 0.6$), all strategy combinations show significant positive synergistic effects, with the $S_1 + S_3$ combination showing the most prominent synergistic effect ($\eta = 3.70$), indicating that optimizing capacity parameters and adding redundant edges give the strongest synergistic enhancement at higher failure ratios. As the failure ratio decreases to $p = 0.7$, the synergistic effect factors of all strategy combinations turn negative, indicating a certain degree of mutual cancellation among strategies in moderate failure scenarios. When the failure ratio further decreases ($p = 0.8$), all combinations again show positive synergistic effects, with $S_1 + S_3$ ($\eta = 1.49$) and $S_2 + S_3$ ($\eta = 1.38$) performing better.

Under deliberate failure: at high failure ratios ($p = 0.9$), only the $S_1 + S_3$ combination shows a significant positive synergistic effect ($\eta = 4.37$), while other combinations show negative or no synergistic effects. At low failure ratios ($p = 0.99$), all strategy combinations show negative synergistic effects, indicating that the joint implementation of multiple strategies actually reduces the overall protection effectiveness when facing minor deliberate failures.

Table 11. The η values under different strategy combinations.

Strategy combinations	Random failure $p = 0.6$	Random failure $p = 0.7$	Random failure $p = 0.8$	Deliberate failure $p = 0.9$	Deliberate failure $p = 0.99$
$S_1 + S_2$	2.20	−0.41	0.05	0	−0.17
$S_1 + S_3$	3.70	−0.13	1.49	4.37	−0.50
$S_2 + S_3$	0.33	−0.35	1.38	−0.93	1.60
$S_1 + S_2 + S_3$	1.72	−0.45	0.70	−0.93	−0.54

5.2. Applicability and cost-effectiveness analysis

To systematically evaluate the economic feasibility of the three robustness optimization strategies in practical applications, we have constructed a decision framework based on unit cost-effectiveness.

The S_1 cost model: capacity optimization involves enhancing the capacity of all nodes and edges in the network. The cost C_1 is defined as: $C_1 = (n_{\text{n}} + n_{\text{e}}) \cdot c_{\text{c}}$, where n_{n} and n_{e} are the numbers of nodes and edges with enhanced capacity, respectively, and C_1 is the unit cost factor for capacity enhancement.

The S_2 cost model: the critical edge protection strategy protects high-betweenness edges in the network through technical means. The cost C_2 is proportional to the number of protected edges: $C_2 = n_{\text{p}} \cdot c_{\text{p}}$, where n_{p} is the number of protected edges and c_{p} is the protection cost per edge.

The S_3 cost model: adding redundant edges requires establishing new physical connections in the network. The cost C_3 is proportional to the number of added redundant edges: $C_3 = n_{\text{r}} \cdot c_{\text{r}}$, where n_{r} is the number of added redundant edges and c_{r} is the construction cost per edge.

Referring to cost analysis in the infrastructure management literature, [40–43] we set the cost ratio relationship among the three strategies as $c_{\text{c}} : c_{\text{p}} : c_{\text{r}} = 1 : 2 : 4$. Let the optimization parameters for S_1 be $\beta = \gamma = 1.1$, and for S_2 and S_3 be $s_{\text{p}} = s_{\text{r}} = 1\%$. Then the S_1 strategy requires optimizing 3000 nodes and 3000 edges, the S_2 strategy requires protecting 30 edges, and the S_3 strategy requires adding 30 edges. From this, we can calculate $C_1 = 300$, $C_2 = 30$, and $C_3 = 60$.

We define the unit cost robustness improvement R_i as the evaluation metric

$$R_i = \frac{\Delta F}{C_i} = \frac{F_{S_i} - F_{\text{base}}}{C_i}, \tag{11}$$

where ΔF is the improvement in the robustness of the network when adopting strategy S_i and C_i is the cost of strategy S_i. Substituting the relevant parameter values, we can obtain the R_i values under different strategies, as shown in Table 12.

Table 12. The R_i values under different strategies.

Strategy	Random failure $p = 0.6$	Random failure $p = 0.7$	Random failure $p = 0.8$	Deliberate failure $p = 0.9$	Deliberate failure $p = 0.99$
S_1	0.00057	0.00191	0.00001	0.00000	0.00069
S_2	0.00268	0.01341	0.00010	0.00000	0.00144
S_3	0.00041	0.00177	0.00004	0.00294	0.00347

From this analysis, it can be concluded that when considering costs, the S_2 strategy should be prioritized under random failure, while the S_3 strategy should be prioritized under deliberate failure.

5.3. Research limitations and future directions

This study assumes that the number of edges in the logistics network equals the number of nodes in the supply chain network (1:1 coupling), which is an idealized fully interdependent structure. In real networks, the correspondence between logistics routes and supply chain nodes is typically more complex, possibly involving one-to-many or many-to-many dependency relationships. Therefore, the system robustness assessed by the model represents a 'theoretical lower bound,' and the actual network resilience may be higher than predicted by the model. Future research can introduce the edge-node quantity ratio (ρ) and many-to-many coupling (ω) as key variables into the model to study the impact of different coupling densities ($\rho \neq 1$) on network robustness, making the model more realistic.

This study assumes a linear relationship between load and degree ($\alpha = 1$). In actual logistics–supply chain networks, load distribution may be influenced by multiple factors such as geographical distance, transportation cost, and time constraints, so the relationship between load and degree may present other forms. Future research can set α to different values to discuss changes in network robustness under nonlinear relationships between load and degree.

The deliberate failure method in this study assumes that attackers have complete knowledge of network topology and failure based on degree/betweenness priority. In reality, attackers may have only partial information or limited failure capabilities. Future research can introduce incomplete information game models to study the game equilibrium between failure and defense strategies.

This study is based on simulation modeling and lacks empirical validation with real logistics–supply chain network data. Future research could obtain industry data to validate the model's predictive capability and perform parameter calibration.

6. Conclusion

This study establishes a logistics–supply chain binary-coupled network (LSBCN) model and systematically investigates network robustness under load redistribution mechanisms using a dynamic load redistribution strategy. We evaluate network robustness under random failures and deliberate failures, thoroughly analyze the impacts of capacity factor (β) and capacity index (γ) on network performance, and design three strategies for robustness optimization: parameter optimization, critical edge protection, and redundant edge addition. Furthermore, we explore the synergistic effects and cost-effectiveness among these strategies.

(1) Regulatory effects of capacity factors on network robustness: for logistics network failures, the capacity factor β_1 exerts a significant influence on overall system robustness. Taking the critical threshold of complete network collapse as the boundary, moderately increasing β_1 rapidly enhances robustness below this threshold, whereas further increases yield limited improvement beyond it. For supply chain network failures, β_2 exhibits distinct characteristics: under random failures, increasing β_2 improves the network size metric F_{W} but has a marginal effect on the GC ratio F_{G}; under deliberate failures, increasing β_2 significantly enhances robustness only when the failure proportion remains below the critical threshold of complete collapse, beyond which the improvement vanishes.

(2) Modulation effects of capacity indices on network robustness: under random failures, the capacity index γ exhibits patterns of influence analogous to β. Under deliberate failures, γ_2 can optimize logistics network robustness to its maximum $F_{\mathrm{W}} = 1$ within a specific interval, while increasing γ_1 consistently enhances robustness during supply chain network failures.

(3) Effectiveness of robustness optimization strategies: Parameter optimization significantly enhances network robustness under both random failures and deliberate attacks, with distinct optimal capacity parameters corresponding to different failure proportions. Critical edge protection effectively improves robustness under random failures, whereas the addition of redundant edges proves more effective under deliberate attacks.

(4) Synergistic effects and cost-effectiveness analysis: under random failures, all strategy combinations exhibit significant positive synergy at high failure proportions ($p = 0.6$), with the combination of parameter optimization and redundant edge addition demonstrating the strongest interaction. At moderate failure proportions ($p = 0.7$), synergy factors turn

negative, whereas at lower proportions ($p = 0.8$) positive synergy reemerges. Under deliberate failures, only the combination of parameter optimization and redundant edge addition shows significant positive synergy at high failure proportions ($p = 0.9$), while all combinations exhibit negative synergy at low proportions ($p = 0.99$). Cost-effectiveness analysis indicates that critical edge protection should be prioritized under random failures, whereas redundant edge addition is preferable under deliberate failures.

Acknowledgments

Lei Zhang acknowledges the support of the National Social Science Fundation of China (Grant No. 23BJY006). Yan-Li Gao acknowledges the support of the National Natural Science Foundation of China (Grant No. 62341306) and Project in JiangXi Province Department of Science and Technology (Grant No. 20232BAB202033). Qiu-Yu Tang acknowledges the support of the Youth Fund Project of Xinjiang under the Ministry of Education Humanities and Social Sciences Research Project (Grant No. 24XJJC630001) and the General Project of the China Society of Logistics (Grant No. 2026CSLKT3-267). Hai-Bo Yu acknowledges the support of the Social Science Research Project of Xinjiang Institute of Technology (Grant No. SY202506).

References

[1] Zhang Z X 2025 *China Journal of Commerce* **34** 143 (in Chinese)
[2] Gu H X, Gu H X and Chen H 2024 *Journal of Jianghan University(Social Science Edition)* **41** 89 (in Chinese)
[3] Yin R R, Yuan H L, Wang J, Zhao N and Liu L 2021 *Physica A* **566** 125600
[4] Meepetchdee Y and Shah N 2007 *International Journal of Physical Distribution & Logistics Management* **37** 201
[5] Zhang X, Liu D, Zhan C J and Chi K T 2017 *IEEE Journal on Emerging and Selected Topics in Circuits and Systems* **7** 228
[6] Buldyrev S V, Parshani R, Paul G, Stanley H E and Havlin S 2010 *Nature* **464** 1025
[7] Wilbanks T J and Fernandez S 2014 *Framing Climate Change Implications for Infr astructures and Urban Systems in Climate Change and Infrastructure, Urban Systems, and Vulnerabilities* (Washington, DC: Island Press) p. 177
[8] Baxter G J, Timár G and Mendes J F 2018 *Phys. Rev. E* **98** 032307
[9] Hu A, Li N, Shi P, Guo H, Zhao H and Yin X 2009 *Economic Geography* **29** 004 (in Chinese)
[10] Radicchi F 2015 *Nat. Phys.* **11** 597
[11] Sun X, Wandelt S and Zhang A 2020 *Journal of Air Transport Management* **89** 101928
[12] Cheng J and Yin P 2022 *Mathematics* **10** 2412
[13] Yan D, Wen J, Du Z, Yang D, Yao W, Zhao H and Liu J 2021 *Power System Protection and Control* **49** 8 (in Chinese)
[14] Wan Z, Su Y Y, Li Z M, Zhang X, Zhang Q and Chen J H 2023 *Ocean & Coastal Management* **245** 106868
[15] Qu S, She Y L, Zhou Q, Verschuur J, Zhao L T, Liu H, Xu M and Wei Y M 2024 *The Innovation* **5** 100653
[16] Gao Y L, Chen S M, Zhou J, Stanley H E and Gao J X 2021 *Physica A* **580** 12136
[17] Wang N, Jin Z Y and Zhao J 2021 *Physica A* **574** 125989
[18] Liu S, Yin C S, Chen D J and Ni S Q 2020 *Plos One* **15** e0239096
[19] Gao Y L, Liang C S and Chen S M 2023 *Control and Decision* **38** 2714 (in Chinese)
[20] Wang J and Huang Y H 2025 *Reliability Engineering & System Safety* **266** 111719
[21] Wu L J, Zou Y L, Wang R R, Yao F and Wang Y 2018 *Complex Systems and Complexity Science* **15** 11 (in Chinese)
[22] Zhang Q, Cao J H, Song T L, Du H D and Zhang C 2021 *Journal of Ordnance Equipment Engineering* **42** 86 (in Chinese)
[23] Xing J C, Chen C X, Zhu Z L and Li Y 2020 *Control and Decision* **35** 3017 (in Chinese)
[24] Wang C, Guo J L and Shen A W 2020 *Systems Engineering and Electronics* **42** 1093 (in Chinese)
[25] Yue D J, Li J H, Zhang J Y and Chen F 2024 *Modern Defence Technology* **52** 61 (in Chinese)
[26] Zhang Y W, Liu W X, Liu G M and Huang S F 2021 *Chinese Journal of Electrical Engineering* **41** 5486 (in Chinese)
[27] Zhao Z, Zhang P and Yang H J 2015 *Physica A* **433** 204
[28] Yu R B, Jiang R, Yan Y W and Hong C 2022 *Journal of University of Electronic Science and Technology of China* **51** 774 (in Chinese)
[29] Gao Y L, Xu W N, Zhou J, Chen S M 2024 *Acta Phys. Sin.* **73** 222 (in Chinese)
[30] Creazza A, Dallari F, and Melacini M 2010 *Supply Chain Management* **15** 154
[31] Liu X M, Stanley H E and Gao J X 2016 *Proc. Natl. Acad. Sci. USA* **113** 1138
[32] Xu X J and Fu X W 2023 *Entropy* **25** 471
[33] Ding C J, Wang Z L and Xu S S 2024 *Symmetry* **16** 736
[34] Gao Y L, Liang C S, Zhou J and Chen S M 2023 *Physica A* **610** 128406
[35] Jiang K L, Liang S B, Liu Y and Zhou L 2025 *Progress in Geography* **44** 1164 (in Chinese)
[36] Gao S and Liu M L 2025 *Logistics Technology* **44** 73 (in Chinese)
[37] Yang L, Liu C Y and Li H 2025 *China Coal* **51** 1 (in Chinese)
[38] Yue J 2025 *Research on the invulnerability of cascade failure of China-Europe f reight train transportation network* (M.Sc. Dissertation) (Dalian: Dali an Jiaotong University) (in Chinese)
[39] Gong W W, Zhou L Y, Xu Z S and Wang Y H 2025 *Railway Technical Innovation* 200 (in Chinese)
[40] Zhang L, Fu L L, Gu W H, Ouyang Y F and Hu Y H 2017 *Transportation Research Part B: Methodological* **105** 378
[41] Lima M S S, Buttgereit A, Queiroz C, Haritonovs V and Gschösser F 2022 *Infrastructures* **7** 32
[42] Lu M, Guler S I and Gayah V V 2024 *Transportation Research Record* **2678** 507
[43] Jin T D, Si S B and Zhu W J 2024 *Frontiers of Engineering Management* **11** 266